GRIPS: a mission with a flavour and a very broad scientific scope

Anatoli F. Iyudin* and GRIPS collaboration†

*Skobeltsyn Institute of Nuclear Physics, Moscow State University, Vorob'evy Gory, 119992 Moscow, Russian Federation
†www.grips-mission.eu

Abstract. The primary scientific goal of the GRIPS mission is to study the early universe using γ-ray bursts. GRIPS, fully described in a paper by Greiner et al. (2008), is a new generation gamma-ray observatory capable of unprecedented spectroscopy over a wide range of γ-ray energies (200 keV–50 MeV) and of polarimetry (200–1000 keV). Scientific goals achievable by this mission are very broad, and include apart of the primary goal also direct measurements of supernova interiors through γ-ray lines from radioactive products of nucleosynthesis, nuclear astrophysics with massive stars and novae, and studies of particle acceleration near compact objects, interstellar shocks, supernova remnants, superbubbles and clusters of galaxies.

Keywords: Compton and Pair creation Telescope; Gamma-Ray Bursts; Early Universe; Gamma-Ray Sources; Nucleosynthesis; Particle Acceleration
PACS: 95.55.Ka, 98.70.Rz, 26.30.-k

A flavour: Stepping beyond classical limits

Gamma-ray bursts (GRB) are the most luminous sources in the sky, and thus act as signposts throughout the Universe. The long-duration sub-group is produced by the explosion of massive stars, while short-duration GRBs likely originate during the merging of compact objects. Both types are intense neutrino sources, and being stellar sized objects at cosmological scales, they connect different branches of research and thus have a broad impact on present-day astrophysics.

Identifying objects at redshift $\gtrsim$6.5 has become one of the main goals of modern observational cosmology, but turned out to be difficult. GRBs offer a promising opportunity to identify high-z objects, and to investigate the host galaxies at these redshifts. GRBs are a factor 10^{5-7} brighter than quasars during the first hour after explosion, and a favourable relativistic k-correction implies that they do not get fainter beyond $z\sim$3. Yet, present and near-future ground- and space-based sensitivity limits the measurement of redshifts at $z\sim$13 (as H-band drop-outs), because GRB afterglows above 2.5 μm are too faint by many magnitudes for 8–10 m telescopes. Thus, a completely different strategy is needed to step beyond redshift 13 to measure when the first stars formed.

[1] GRIPS is a proposal submitted in response to the ESA Cosmic Vision Call in June 2007.

Fortunately, nuclear physics offers such a new strategy. Similar to X-ray and optical absorption lines due to transitions between electronic levels, resonant absorption processes in the nuclei exist which leave narrow absorption lines in the γ-ray range. The most prominent and astrophysically relevant are the nuclear excitation (element-specific narrow lines at 5–9 MeV), the Giant Dipole resonance (GDR; proton versus neutron fluid oscillations; $\sim$ 25 MeV; two nucleons and more) and the Delta-resonance (individual-nucleon excitations, 325 MeV; all nucleons, including H!). Such resonant absorption only depends on the presence of the nucleonic species, and not on ionization state and isotope ratio. They imprint well-defined spectral features in the otherwise featureless continuum spectra of GRBs (and other sources). This is completely new territory (Iyudin et al. 2005), but with the great promise to measure redshifts directly from the gamma-ray spectrum!

Technically, this new strategy requires sensitive spectroscopy in the 0.2–50 MeV band. The detection of GRBs requires a large field of view. Therefore, the logical detection principle is a Compton telescope. In addition, such detectors can be tailored to have a high polarisation sensitivity. Polarimetry is the last property of high-energy electromagnetic radiation which has not been utilized in its full extent, and promises to uniquely determine the emission processes in GRBs, as well as many other astrophysical sources. With its large field of view, such a detector will not only scan 80% of the sky within one satellite orbital period of 96 min., but also provide enormous grasp for measuring the emission produced by different type compact system (X-ray binaries, X-novae, μQSOs, pulsars, SGRs) activity, or by explosive nucleosynthesis, and/or as a result of cosmic-ray acceleration and consequent interaction with the surrounding medium.

Main goal of the mission

GRIPS aims at a detection of gamma-ray bursts at redshifts above 13. This will allow us to explore rather directly the universe in the epoch where first stars formed.

High-redshift GRBs: GRB afterglows are bright enough to be used as pathfinders to the very early universe. Since long-duration GRBs are related to the death of massive stars, it is likely that high-z GRBs exist. Theoretical predictions range between few up to 50% of all GRBs being at $z > 5$ (Lamb & Reichart 2001, Bromm & Loeb 2002), and stellar evolution models suggest that 50% of all GRBs occur at $z > 4$ (Yoon et al. 2006). The polarisation data of the Wilkinson Microwave Anisotropy Probe (WMAP) indicate a high electron scattering optical depth, hinting that the first stars formed in the range $20 \lesssim z \lesssim 60$ (Kogut et al. 2003, Bromm & Loeb 2006, Naoz & Bromberg 2007). GRIPS is designed to measure GRBs from the death of these first stars and probe the universe up to the highest redshifts after matter-photon decoupling.

Redshift determination via resonance absorption: The observational use of nuclear resonance absorption for GRB redshift determination depends on two critical questions: "Is there enough matter along the sight lines to GRBs?", and "Is the resulting absorption detectable?".

Is there enough matter along the sight lines to GRBs? Apart from galactic foreground

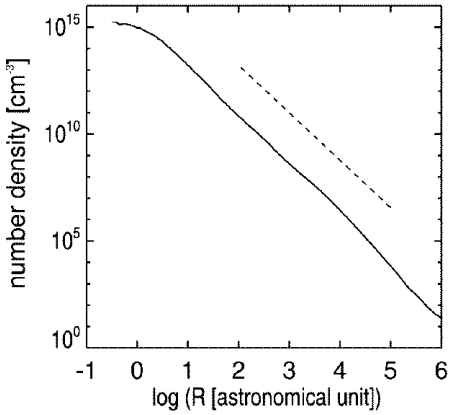

FIGURE 1. Radial density around a GRB progenitor at a redshift z=19. The density profile is close to a power law $\propto R^{-2.2}$ (dashed line). It contains about 10^{28} cm^{-2} column density within the inner 1-2 AU, and further 10^{28} cm^{-2} in each shell from 2-10, 10-100, 100-1000 AU! (From Yoshida et al. 2006)

extinction, relatively little intrinsic extinction has been found in the afterglow spectral energy distributions of GRBs, both at X-rays and at optical/NIR wavelengths. Yet, there is evidence, both theoretical as well as observational, that there is substantial amount of matter along the line of sights to GRBs. This applies to the local GRB surrounding as well as to the larger environment of the host galaxy in which the GRB explodes. Temporally variable optical absorptions lines of fine-structure transitions indicate that (i) all material at distances within a few kpc is ionized, most likely by the strong UV photon flux accompanied with the emission front of the GRB, and (ii) beyond this ionized region the absorbing column is still at a level of 10^{21} cm^{-2} (Schady et al. 2007; Vreeswijk et al. 2007). Thus, present-day capabilities of the optical/NIR as well as X-rays measurements are not adequate to determine the density of local matter around GRBs. However, at γ-rays this matter will be detectable via nuclear resonance absorption even when this matter is completely ionized: the GRB gamma-ray radiation has to pass through it - and it will suffer resonance absorption independent of the matter ionization state.

A variety of theoretical simulations of GRB progenitors have been made (e.g. Bate, Bonnell & Bromm 2003, Yoshida et al. 2006, Abel et al. 2007, Gao et al. 2007), pertaining to the formation of the first stars, the fragmentation rate, and density structure around the first star. The resulting mass of the star as well as the density structure are difficult to predict because they depend on the collapse conditions (merger or not, strength of winds, etc). However, it is important to realize that some simulations in fact predict column densities of up to 10^{29} cm^{-2} around the first stars (Yoshida et al. 2006, Spolyar et al. 2008; see also Fig. 1)! It remains to be observationally demonstrated whether the conditions modelled in these simulations are realized. Yet, the existence of what one "normally" would refer to as "unbelievably high" column densities is plausible – note that even pristine and fully-ionized hydrogen imprints resonant absorption!

GRBs are the best and possibly the only tool to measure such conditions.

Is the resulting absorption detectable? This question can be subdivided into two issues: Firstly, are there astrophysical conditions which favour large line of sight columns, but not excessively large densities? If the density is too high, multiple-scattering of higher

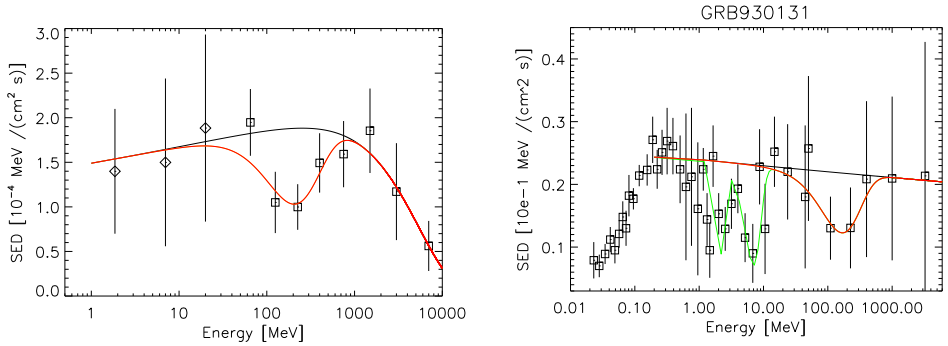

FIGURE 2. **Left:** 3C 279 spectrum during the January 1996 flare as measured by COMPTEL (diamonds) and EGRET (squares), which includes the Δ resonance absorption in the circumnuclear environment (red line) in addition to a cut-off power law (black line). The best-fit energy for the Δ resonance is 208 ± 25 MeV, implying a redshift 0.57 ± 0.12, close to the optically determined z=0.536. **Right:** Fit to the combined COMPTEL/EGRET spectrum of GRB 930131. The throughs at 5–8 MeV and 100–200 MeV are compatible with the Giant Dipole and Delta resonance, respectively, at a redshift of z$\sim$0.6 (Iyudin et al. 2007b).

energy photons could partly fill the energy window of a resonance, thus smearing the absorption trough. This may happen via Compton scattering or the cascading of high-energy photons. Inspite of cross sections for Compton scattering being about a factor of 30-40, and for pair production of about factor of 8 for hydrogen and helium, larger than the peak cross section of the Giant Dipole or Delta Resonance, the jet geometry in GRBs, as well as in blazars, over-compensates for this disparity: *it is the differential cross section that matters*. At the Dipole Resonance energy, the Compton-scattered photon beam has a FWHM of 16°, or 0.5 sr. For a 1° opening angle of the jet, the resulting GDR absorption of the beam photons is a factor $\sim$12 more efficient than the Compton re-scattering of higher energy continuum photons into the beam. In addition, Compton scattering leaves the energy of the scattered photons in a quite broad energy range, much greater than the width of the resonance - this adds another factor of E/ΔE ($\gtrsim$3 for the GDR) in favor of the resonance absorption. For pair production, only the latter effect comes into play. Furthermore, even in high-density environments, there are two possibilities which alleviate the problem of re-filling: (i) the transverse dimension of the absorber is less than $\sim$1.5 attenuation lengths at the energy of the highest attenuation value (Varier et al. 1986) or (ii) the absorber consists of many clumps (clouds) of matter, a solution which has been proposed to explain the UV and X-ray (Arav et al. 2003; 2005) or IR emission (Elitzur et al. 2004) in optically thick absorbers around AGN. First hints for resonance absorption in few cases of flaring AGNs (Fig. 2, left panel; Iyudin et al. 2005), and GRBs (Fig. 2, right panel) at the 2σ level have been found based on COMPTEL and EGRET data.

Secondly, how narrow/broad will the resonant absorption features be at different redshifts, and what is the required energy resolution and sensitivity to detect them? Fig. 3 shows the rest-frame resonance absorption lines for two different metallicities of absorbers which clearly illustrate a starkly different relative intensity ratios of absorption troughs. The GDR around 25 MeV has a FWHM $\sim$ 10 MeV, thus $\sim$300 keV resolution

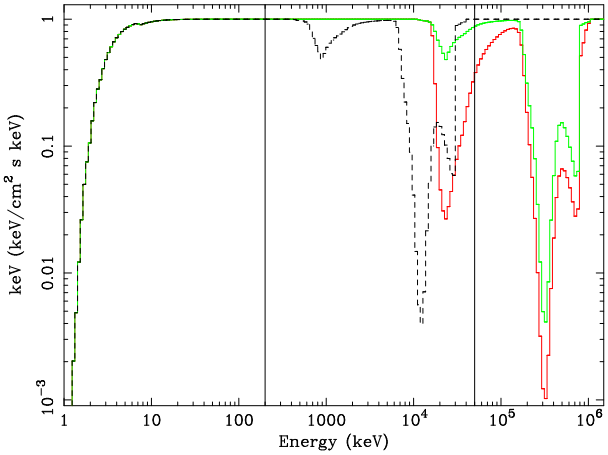

FIGURE 3. Resonance absorption lines for two different redshifts (black: z=25; color: z=0) and different metallicities: Z=0.1 (green) and Z=1 (red) solar metallicity. Note the obvious difference in the relative strengths of the absorptions. The solid vertical lines bracket the energy band of GRIPS from 200 keV to 50 MeV. A total column of 10^{28} cm^{-2} has been assumed to clearly visualise the effect, and a density smaller than 10^5 cm^{-3} to avoid refilling of the lines due to scattering. The detectability of these resonance lines with the proposed instrument is achieved down to column densities of 10^{25} cm^{-2}.

of GRIPS at 10 MeV is fully sufficient to properly resolve the feature. The goal of GRIPS is to measure those resonance absorptions at redshifts $z \sim 13-30$. Full simulations for the γ-ray instrument on GRIPS show that column densities of $10^{26}...10^{27}$ cm^{-2} will be detectable for $\sim$ 30–40% of all GRBs seen in spectroscopy mode, and those with as little as 10^{25} cm^{-2} for the 10% brightest GRBs (see also Fig. 10).

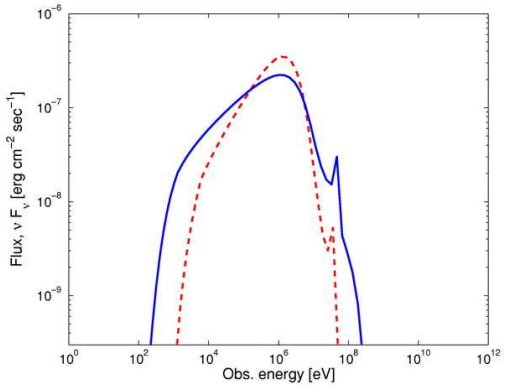

FIGURE 4. Spectra averaged over the GRB duration, obtained for high compactness l. The two models assume Γ=300, L = 10^{52} erg, z = 1, and differ in the variability timescale of δt = 10^{-4} s, (blue solid line; implied l=250); and δt = 10^{-5} s (dashed line; l=2500) at which the Lorentz factor Γ varies. The scattering optical depth at the end of the dynamical time is 13 and 56, respectively. The peaks observed at $\sim$80 MeV result from pair annihilation which is larger for larger compactness. (From Pe'er & Waxmann 2004)

These features have not been seen before in EGRET TASC, BATSE SD, or COMPTEL (D2) data due to the combination of insufficient sensitivity, poor energy resolution and pre-canned response matrices for fixed energy bins. GRIPS with its enhanced sensitivity, energy resolution and a large FOV in one instrument is capable to detect nuclear

resonance troughs in the spectra of a large number of sources.

If the GRB environment contains total (neutral plus ionized) column densities of 10^{25} cm^{-2} or higher, GRIPS will be able to measure redshifts via the nuclear resonance absorption directly from the γ-ray spectrum, and thus be sensitive well beyond z$\sim$13.

What are the energetics of GRBs? There is increasing evidence, both observational (Starling et al. 2005) and from theory (Woosley et al. 2006) that a GRB may launch two jets: one highly relativistic ($\Gamma > 200$, kinetic energy of 10^{51} erg), central jet with an opening angle of a few degrees, and a broader jet with sub-relativistic ejecta (0.1c, kinetic energy 10^{52} erg) spread over 1 radian. The underlying physical basis of the correlation between the isotropic equivalent energy emitted in the prompt radiation phase and the peak energy (E_{peak}) of the measured spectrum (Amati et al. 2002, Ghirlanda et al. 2004) is mysterious. Measuring the Lorentz factor Γ from the γ-ray emission itself with GRIPS would provide a major step in understanding the cause of this correlation and in determining the energetics of GRBs.

Numerical models of the prompt emission due to internal shocks in an expanding relativistic wind exist in many different variants. In most of these, the spectrum is expected to significantly deviate from an optically thin synchrotron spectrum. A time-dependent calculation which includes cyclo-synchrotron emission and absorption, inverse and direct Compton scattering, and e^+e^- pair production and annihilation has shown (Pe'er & Waxman 2004) that (i) (in-flight) annihilation emission lines are expected at surprising strength (Fig. 4), and (ii) thermal Comptonization leads to emission peaking at $\gtrsim$30 MeV, possibly explaining the additional MeV component seen in GRB 941017 (González et al. 2003). The annihilation line will be boosted by Γ into the $\gtrsim$100 MeV range, but adiabatic energy losses as well as GRB cosmological redshift lowers the observed photon energy back into the few MeV band. Thus, once the redshift is determined by the resonance lines (or ground-based optical/NIR telescopes for z$<$13), the measured energy of the annihilation line allows a direct determination of the Lorentz factor from the prompt gamma-ray emission spectrum. GRIPS will allow us to measure the Lorentz factor of the prompt γ-ray burst emission via the predicted annihilation line, and thus directly measure the total energy of the explosion for at least 15% of all GRBs. Since the measured annihilation line energy is proportional to the ratio Γ/z, GRIPS can detect the line in the range ($0.5 \gtrsim \Gamma/(1+z) \gtrsim 100$), thus covering the full predicted range of Γ (50–1000) and z (0.5-60).

What is the emission mechanism?

Spectra: Based on the knowledge gained from observation in the keV-MeV range several possible radiation mechanisms exist, all of which produce characteristic spectra in the super-MeV range. Two main classes of models (see Mészáros 2006) have been discussed. (1) Synchrotron/inverse Compton emission of electrons and protons: It is very probable that particles are accelerated to very high energies close to the emission site. This could either be in shock waves, where the Fermi mechanisms or other plasma instabilities act, or in magnetic reconnection sites. Therefore, it is likely that the observed emission in the keV range scatters on these relativistic electrons, which will result in inverse Compton emission in the super-MeV domain. This occurs in both internal and external shock scenarios. Furthermore, most of the outflow energy, transported by the protons will predominantly be in the super-MeV range. (2) Hadron related emission via pion production and cascades: High-energy, neutral pions (π^0) can be created as

shock-accelerated, relativistic protons scatter inelastically off ambient photons ($p\gamma$ interactions). These later decay into γ-rays. This is, e.g., suggested to occur in GRB 941017 (González et al. 2003). Similarly, if the neutrons in the outflow decouple from protons, inelastic collisions between neutrons and protons can produce pions and subsequent high-energy emission.

The spectra of some GRBs alternatively have been well fit by both the Band model and a combination of a black body plus power law model (Ryde 2005; McBreen et al. 2006). Rees & Meszaros (2005) suggested that the E_{peak} in the γ–ray spectrum is due to a Comptonised thermal component from the photosphere, where the comoving optical depth falls to unity. The thermal emission from a laminar jet when viewed head–on would give rise to a thermal spectrum peaking in the X-ray or γ-ray band. The resulting spectrum would be the superposition of the Comptonised thermal component and the power law from synchrotron emission. Thus, from theory there is no indication that GRB spectra should deviate from a smooth continuum, and thus can be used as reliable background light sources for nuclear absorption features.

GRIPS will measure the broad-band spectra of $\sim$660 GRBs/yr from 100 keV – 50 MeV with 3% energy resolution. GRIPS will distinguish between the various, contradictory mechanisms by covering the transition from the classical keV into the dozen MeV regime.

Polarisation as a diagnostic of the GRB emission mechanism: The link between the γ-ray production mechanism in GRBs and the degree of linear polarisation can constrain models. A significant level of polarisation can be produced in GRBs by either synchrotron emission or by inverse Compton scattering. The fractional polarisation produced by synchrotron emission in a perfectly aligned magnetic field can be as high as 70–75%. An ordered magnetic field of this type would not be produced in shocks but could be advected from the central engine (Granot & Königl 2003, Granot 2003, Lyutikov et al. 2003). It should be possible to distinguish between Synchrotron radiation from an ordered magnetic field advected from the central engine and Compton Drag. Only a small fraction of GRBs should be highly polarised from Compton Drag because they have narrower jets, whereas the synchrotron radiation from an ordered magnetic field should be a general feature of all GRBs.

GRIPS will allow us to measure the polarisation of the prompt γ-ray burst emission to a few percent accuracy for about 10% of all detected GRBs. Moreover, the superior polarisation sensitivity will securely measure whether or not the percentage polarisation varies with energy, angle and/or time over the burst duration of a dozen brightest GRBs.

Garanteed science with GRIPS

GRIPS will address other, non-GRB science topics, and lead to guaranteed science returns. Major science topics are (a) to unveil the physics of stellar explosions, and (b) to illuminate the physical processes which lead to particle accelerations from thermal up to relativistic (cosmic-ray) energies.

With the imminent launch of NASA's GLAST Observatory (30 MeV - 100 GeV) and the long-term continuation of ESA's INTEGRAL Observatory (20 keV - few MeV)

there will be a dramatic lack of coverage of the gamma-ray sky in the 1-30 MeV range. GLAST will detect thousands of new sources, while the only existing MeV data (from GRO/COMPTEL) is for a handful of very bright ones. The discovery potential is clearly enormous. At present, multiwavelength spectra of the majority of sources have a notable absence of data at MeV energies, although often the main power is expected there. Without a mission like GRIPS, the MeV sky with its wealth of astrophysics will be less well known even than the TeV sky (via the new Cerenkov observatories), which is a quite disillusioning prospect.

Variety of γ-ray sources to study with GRIPS

Blazars: Recent Swift/BAT observations find many blazars with very flat (photon index 1.6–1.8) spectra in the 20–150 keV range, and extrapolations indicate that all of those will be securely detectable by GRIPS. The measurement of the resonance absorption will substantially help in the identification process, since the redshift will be known from the gamma-ray spectra (Iyudin et al. 2005, 2007a). Gamma-ray polarization can be measured for the flare states. Comparing with radio polarization and multi-wavelength light-curves, this will pin down the origin of the γ-ray flares (Wehrle et al. 2001; Jorstad et al. 2006).

Pulsars, AXPs, and SGRs: Pulsars are an excellent laboratory for the study of particle acceleration, radiation processes and fundamental physics in environments characterized by strong gravity, strong magnetic fields, high densities and relativity. Above ~ 50 MeV EGRET has detected 6-10 pulsars and candidates (Hartman et al. 1999), and Schönfelder et al. (2000) reported for the COMPTEL survey 4-5 pulsars corresponding to EGRET detections and one high-magnetic field pulsar (PSR B1509-58) with emission up to 30 MeV. Estimates for the number of possible pulsar detections by future, more sensitive, gamma-ray instruments are based on our empirical knowledge of pulsar efficiencies and spectra, new radio surveys that now contain about 2000 pulsar detections, and on the extrapolations afforded by theories of high-energy emission from rotating, magnetized neutron stars. These theories are still quite disparate. For energies above several 10 MeV and for the sensitivity of the Large Area Telescope on GLAST, predictions range from ~ 60 detections (Harding 2007) to about 800 (Jiang & Zhang 2006), with several predictions between 120 and 260 pulsars. Many of these pulsars are so-called 'radio-quiet' objects comparable to the Geminga pulsar. Additional predictions for about 100 millisecond-pulsars have been published for GLAST by Story et al. (2007). GRIPS' sensitivity for wide band spectra above ~ 10 MeV (normal pulsars) and below 1 MeV (high B-field pulsars and AXPs) exceeds the COMPTEL sensitivity by a similar factor that holds when going from EGRET to GLAST. From the EGRET/COMPTEL relation we therefore estimate the number of GRIPS pulsars to be about 50-70% of the GLAST pulsars and expect to detect 60-70 pulsars in the GRIPS energy range > 10 MeV. GRIPS-determined light curves and phase-resolved spectra in the 1–50 MeV range will provide decisive insights into the pulsar magnetosphere and the acceleration processes located there. Polarisation is a unique characteristic of particles radiating in strong magnetic fields. Pulsars and their surrounding pulsar wind nebulae (PWN) are highly polarised. GRIPS will be sensitive enough to measure polarisation below a few MeV from several pulsars.

'Magnetars' appear to observers in the forms of 'anomalous X-ray Pulsars' (AXP) or, possibly related, 'soft gamma-ray repeaters' (SGR). Pulsed radiation with a thermal

spectrum at soft X-rays (1–10 keV) and an extremely hard power-law up to nearly 1 MeV has been observed from 6-8 AXPs (Kuiper et al. 2006). The continuous all-sky survey of GRIPS promises to capture unique data for high-energy neutron star astrophysics.

XRBs, X-ray novae There is a large chance for GRIPS to serendipitously detect a transient compact object, or binary system, in an active phase in the Galaxy, or in the Local Group. The estimates of the frequency of such events is rather uncertain. But, if XRB will be caught by GRIPS in an outburst state the broad spectral coverage, and excellent timing properties of GRIPS will allow to scientific community to digest an excellent set(s) of a data, that will make conclusions possible on the dominant emission mechanism, power spectral density (PSD), as well as on the relation of the spectral state to the PSD of the object.

Superbubbles: Massive stars in the Galaxy appear in groups (e.g. OB associations), such that their strong wind and supernova activity overlaps and generates large superbubbles (SBs). Interacting shocks within the superbubble thus provides a natural environment for cosmic ray accerelation (GCRs). GRIPS has sufficient sensitivity to test the theory of galactic cosmic ray acceleration in the SB environment by observing galactic SBs as well as 30 Dorado in the LMC in gamma-ray line emission. Lines of $^{12}C^{*}$ and of $^{16}O^{*}$ at 4.44 MeV, and 6.1 MeV, 6.97 MeV, and 7.17 MeV, respectively, would be the best indicators of the CR acceleration in the SB.

Diffuse continuum MeV gamma-ray emission from the interstellar medium arises from the interactions of cosmic-ray electrons with interstellar matter and radiation fields. Bremsstrahlung on atomic and molecular hydrogen produces gamma-rays with energies typically half of the electron energy, so that gamma-rays in the GRIPS range trace electrons in the 1-100 MeV ranges. At these energies direct cosmic-ray measurements are virtually impossible because of the large solar modulation; synchrotron radiation occurs at frequencies too low to be observable. Hence GRIPS gamma-ray observations are our only window to interstellar electrons at MeV energies. Inverse-Compton scattering of 100-1000 MeV electrons and positrons on interstellar radiation is an important component of continuum gamma-rays, and dominates at low energies. In fact, recently this component has been shown to explain most of the diffuse emission from the Galactic ridge observed by INTEGRAL (Porter et al. 2008). Both primary and secondary cosmic-ray electrons and positrons contribute to this emission, and hence observations in this part of the spectrum give valuable information on high-energy particles in the Galaxy. On the other hand this process fails to explain all of the diffuse emission observed by COMPTEL (Strong et al. 2005, Porter et al. 2008), suggesting a possible contribution from populations of unresolved hard gamma-ray sources, like AXPs and radio pulsars. GRIPS can trace and disentangle those components towards higher energies.

Solar flares accelerate ions to tens of GeV and electrons to tens of MeV. GRIPS would obtain high-statistics time-resolved spectra, permitting precise measurements of the hard-X ray continuum from accelerated electrons, of tens of strong nuclear lines and of the high-energy emission from π^0 decay and $\pi^{\pm}$-decay leptons. This, for the first time, would allow detailed studies of the evolution of the energy spectra and composition of the accelerated particles which are the key properties for the understanding of the acceleration mechanism and the transport of energetic particles in solar flares. In particular, it will be possible to determine the accelerated ^{3}He/^{4}He ratio and the heavy-ion content of the interacting particles and compare them with observations of solar energetic particles

in interplanetary space, where large overabundances of ^{3}He ($\approx$ 100 - 1000) and of low-FIP elements ($\approx$ 10-30) are found after impulsive-type flares. Additional information would come from polarization measurements of the bremsstrahlung continuum and of some nuclear lines and the detection of delayed X- and γ-ray line emission from solar active regions that are following the production of relatively long-lived radio-isotopes during strong flares (Tatischeff et al. 2006).

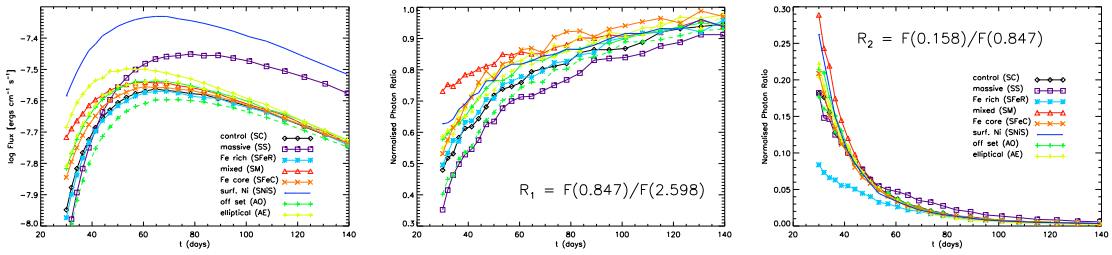

FIGURE 5. SNIa model light curves in the 0.1-3.5 MeV band for a 1 Mpc distance, and time since explosion (left), as well as ratios of gamma-ray lines from ^{56}Ni decay (middle and right) which provide an important diagnostics of the inner supernova and the explosion mechanism. Shown are spherically-symmetric models as well as two cases of asphericities (AO and AE) which represent the extremes with respect to viewing angle. The high-energy lines provide a sensitive diagnostics to asphericities of the SN. (From Sim & Mazzali 2008)

Nuclear astrophysics

Supernovae of Type Ia - the cosmological candle?! SNIa are considered on purely empirical grounds to be standardizable candles; no physical explanation could be established for the homogeneity of thermonuclear disruptions of white dwarf stars, which is the widely-accepted model. In view of the far-reaching cosmological implications of the SNIa apparent dimming in the distant universe, it remains a major concern for supernova scientists (Leibundgut 2001, Branch & Nomoto 2007). Phrased at an extreme: dark energy might not exist at all, if our estimates of SNIa properties across cosmic times or selection biases are inadequate! Already a 7% Ibc contamination level is sufficient to produce $\Omega_\lambda = 0.7$ from no effect (Homeier 2005). Thus, understanding the physics of SNIa is of outmost importance. GRIPS will provide the data for a physical understanding of the "Phillips relation" and the related errors. Due to the huge dynamic scales in time and space of the relevant physical processes, numerical simulations must make use of approximations. Guidance from observations is essential in building a physical model. Most direct access to isotope information is through nuclear lines emitted from radioactive decays, which can provide kinematic information from partially-embedded freshly-synthesized species. Penetrating γ-rays are expected to escape from the supernova as early as a few days after the explosion. GRIPS will detect all lines from ^{56}Ni decay chain to ^{56}Fe , including γ-ray lines at 158 keV (from ^{56}Ni, early and probably occulted) and at 847, 1238, 1771 and 2598 keV. Line shape and centroids reflect the original ^{56}Ni kinematics, line ratios are a key diagnostic of the explosion morphology and hence model types. Recent SNIa surveys record $>$10 nearby events ($<$50 Mpc), which will be detected by GRIPS in the energy range of the (direct and scattered) ^{56}Ni decay γ-ray range up to $\sim$2.5 MeV at $\sim$100 days after explosion, when the SN is transparent to gamma-rays (see Sim & Mazzali 2008). In addition to an absolute determination of the ^{56}Ni amount from the γ-ray line flux, due to its broad energy range, line ratio diag-

nostics will be provided by GRIPS, that will measure at least one SNIa per year, thus significantly enhancing the sample of SNIa with meaningful γ-ray constraints.

Massive-star nucleosynthesis is responsible for most of the intermediate-mass elements from oxygen through iron (Woosley & Weaver 1995; Heger et al. 2003). Different fusion episodes from hydrogen through silicon burning in shells of the rapidly-evolving star after its core-hydrogen burning phase (main sequence), plus nucleosynthesis in the supernova following the final gravitational collapse of the star, are responsible for this element production. The complexities of stellar-structure evolution and active nuclear-reaction networks are difficult to model. Beyond the (abundant, but rather indirect) observations of elemental abundances through atomic lines, only measurements of the key isotopes through their radioactive decays can provide calibrators for those models.

A key isotope for supernova-interior nucleosynthesis is ^{44}Ti with a decay time of $\sim$85 years, a γ-ray line at 1157 keV and X-ray lines at 68 and 78 keV. This radioactive decay has been observed from the Cas A supernova remnant (Iyudin et al. 1994, Vink et al. 2001). Its abundance and kinematics directly arises from the processes of accretion and fall-back onto the central remnant. This otherwise unaccessible inner region of a core collapse is at the origin of gamma-ray burst formation by massive stars (The et al. 2006). GRIPS will deepen surveys for ^{44}Ti gamma-ray sources (1.16 MeV) in the Galaxy within a 5-year mission down to 6×10^{-7} ph cm^{-2} s^{-1}, and should detect 10-15 remnants if ^{44}Ti ejection is typical for core-collapse supernovae (see The et al. 2006). Furthermore, detection of MeV continuum in core-collapse SNe, and especially in the Ib/c class, would indicate that a fraction of the relevant kinetic energies liberated in these explosions is conveyed to the acceleration of electrons to very high energies and to the re-emission through the synchrotron process, illuminating our understanding of the GRB-powering mechanisms in SNe.

For a sufficiently nearby (less than 100 Mpc) SN associated with a GRB, prompt gamma-ray spectroscopy of early ^{56}Ni lines at 158 keV and 812 keV would be another unique opportunity to calibrate model of the core-collapse SNe, considering the predicted gamma-ray flux near the time of transparency ($\sim$50-100 days) (see Sim & Mazzali 2008). GRIPS is the only foreseeable monitor to study broad continuum and radioactivity MeV gamma-rays from nearby core-collapse supernovae, with these unique signatures.

There are two more important tracers to study the massive stars nucleosynthesis. One is ^{26}Al isotope that is predominantly produced by massive stars (Prantzos & Diehl 1996), with nucleosynthesis in early stages of core hydrogen burning and in late shell burning stages plus supernova nucleosynthesis (Limongi & Chieffi 2006). The ^{60}Fe isotope is another tracer, that is produced in late burning stages of massive stars, and is ejected by the supernova. Both isotopes are decaying on a scale of $\sim$ My, and their production over My time scales is accumulated and can be observed in the γ-ray lines.

With a 5-year survey sensitivity of $\sim6\times10^{-7}$ ph cm^{-2} s^{-1}, GRIPS will map the Galaxy in ^{60}Fe radioactivity gamma-rays for the first time at several degrees spatial resolution and will deepen the Galactic survey for ^{26}Al (see Diehl et al. 2006).

Novae: GRIPS will detect several Galactic novae through annihilation emission, that will make possible to combine positron annihilation with ^{7}Be and ^{22}Na diagnostics to understand the nova ignition and burning process.

Positron Astrophysics: Imaging of the γ-ray emission from the annihilation of positrons

with INTEGRAL/SPI (Knödlseder et al. 2005) has revealed a new major puzzle: The expected sources of positrons in the Galaxy are predominantly located in the disk of the Galaxy, while the Galactic bulge is by far the brightest observed feature in annihilation γ-rays. This initiated a quest for new types of candidate positron producers, ranging from the annihilation of dark matter particles accumulated by the Galaxy's gravitational field (Hooper & Wang 2004), to the large-scale transport of positrons from their disk sources through the Galactic halo into the central bulge before their annihilation (Prantzos 2004), or significant diffusion of positrons generated by past activity and energetic proton ejection from the central black hole in our Galaxy (Cheng et al. 2006).

GRIPS will help to clarify the validity of such extreme models, as it will be sensitive to the full spectral range of annihilation emission (300→511 keV, and above, for annihilations-in-flight). With its angular resolution of $\sim 3.^{\circ}5$ at 511 keV, GRIPS will map the bright bulge emission of positron annihilation and its merging with the disk component.

Overview of instruments

GRIPS will carry two major telescopes: the Gamma-Ray Monitor (GRM) and the X-Ray Monitor (XRM). The GRM is a combined Compton scattering and Pair creation telescope for the energy range 0.2–50 MeV. It will thus follow the successful concepts of imaging high-energy photons used in COMPTEL (0.7–30 MeV) and EGRET (>30 MeV) but combines them into one instrument. New detector technology and a design that is highly focused on the rejection of instrumental background will provide greatly improved capabilities. Over an extended energy range the sensitivity will be improved by at least an order of magnitude with respect to previous missions (Fig. 7) and the large field of view, better angular and spectroscopic resolution of GRM allows the scientific goals outlined in this project to be addressed. The XRM is based on the mature concept and components of the eROSITA X-ray telescope, which is scheduled for a space mission on the Russian platform Spektrum-XG (Predehl et al. 2006, Pavlinsky et al. 2006).

Gamma-Ray Monitor

Two physical processes dominate the interaction of photons with matter in the γ-ray energy band from 200 keV to $\sim$50 MeV: Compton scattering at low energies, and electron-positron pair production at high energies, with the changeover at $\sim$ 8 MeV for most detector materials. In both cases the primary interaction produces long-range secondaries whose directions and energies must be determined in order to reconstruct the incident photon. The GRM, like previous Compton and pair creation telescopes, will employ two separate detectors to accomplish this task: a tracker (D1), in which the initial Compton scatter or pair conversion takes place, and a calorimeter (D2), which absorbs and measures the energy of the secondaries. In the case of Compton interactions, the incident photon scatters off an electron in the tracker. The interaction position and the

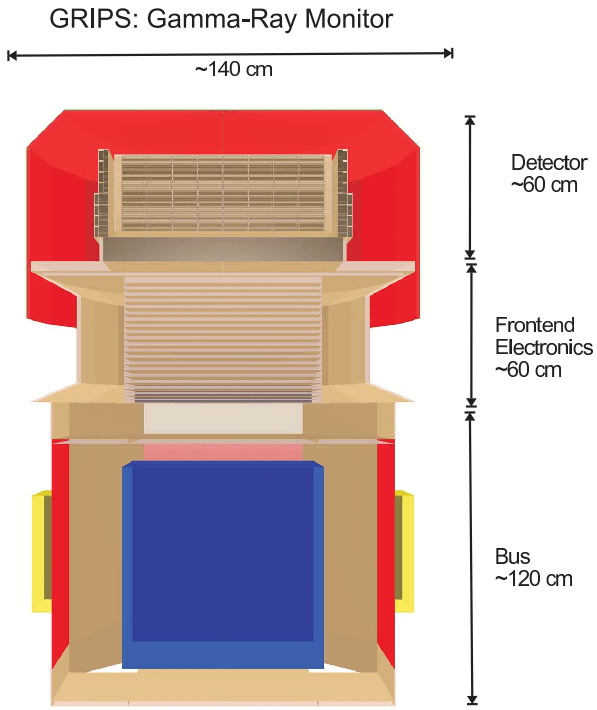

FIGURE 6. Expected size and assembly of the Gamma-Ray Monitor and related electronics on the satellite bus as included in the GEANT model of the GRM.

energy imparted to the electron are measured. The scattered photon interaction point and energy are recorded in the calorimeter. From the positions and energies of the two interactions the incident photon angle is computed from the Compton equation. The primary-photon incident direction is then constrained to an event circle on the sky. For incident energies above about 2 MeV the recoil electron usually receives enough energy to penetrate several layers, allowing it to be tracked. This further constrains the incident direction of the photon to a short arc on the event circle. GRM will determine GRB locations to better than 1°(radius, 3σ).

The differential Klein-Nishina cross-section for Compton scattering contains a strong dependence on the polarization of the incident γ-ray photon. Scattered photons are emitted preferentially perpendicular to the direction of the electric field vector of the incoming photon. The strongest azimuthal modulation in the distribution of scattered photons will be achieved for low gamma-ray energies and Compton scatter angles around 90°. This will make a Compton telescope with a calorimeter covering a large solid angle a unique polarimeter. In the case of pair production, the incident photon converts into an electron-positron pair in the tracker. These two particles are tracked and determine the incident photon direction. The total energy is then measured through the deposits absorbed in the tracker and/or the calorimeter.

In addition to the 'telescope-mode' described above, the D2 detectors can also be read out in the so-called 'spectroscopy-mode' i.e. recording interactions that deposit energy only in the calorimeter. Using the side walls and the bottom of D2 as separate units a coarse localization and high-quality spectra of GRB events can be obtained. This mode

of operation follows the example of BATSE and the EGRET-TASC on CGRO, the lateral shields of the Phoswich Detector System on Beppo-SAX, and the GBM on GLAST.

GRM design and simulations The design of a new high-energy γ-ray telescope must be based on numerical simulations as well as experimental detector developments. The baseline design and input to the Monte-Carlo simulations of the GRM is shown in Fig. 6. The top part shows the detector head with the central stack of double-sided Si-strip detectors (tracker D1) surrounded by the pixellated calorimeter (D2) and an anticoincidence system (ACS) made of plastic scintillator. The simulations were carried out with the MGGPOD suite (Weidenspointner et al. 2005), which allows for a detailed simulation of the primary and secondary (activation) background in the chosen low-earth orbit. The modeling of the instrument functions, the reconstruction of the Compton and pair data, and the final performance calculations were carried out with the MEGAlib software suite (Zoglauer et al. 2006) which had been developed in the course of the MEGA prototype development (Andritschke et al. 2005).

Below the γ-ray detector is the GRM electronics and a generic spacecraft bus. In the simulations the bus of the Advanced Compton Telescope study was used (Boggs et al. 2006).

The D1 detector consists of 64 layers each containing a mosaic of 8×8 double-sided Si strip detectors of area $10 \times 10\,\mathrm{cm}^2$. The layers are spaced with 5 mm distance. The D2 calorimeter is made of $LaBr_3$ prisms ($5 \times 5\,\mathrm{mm}^2$ cross-section) which are read out with Si Drift Diode (SDD) photodetectors. The upper half of the D2 side walls feature scintillators of 2 cm length and the lower half has 4 cm thick walls. The side wall crystals are read out by one SDD each. The bottom calorimeter is 8 cm thick and is read out on both ends of the crystals to achieve a depth resolution of the energy deposits.

The whole detector is surrounded by a plastic scintillator counter that acts as an anti-coincidence shield (ACS) against charged particles. Read out of the scintillation light, which is collected with embedded wavelength-shifting fibers to ensure the ACS uniformity, will be done with Si APD detectors.

Most of the structural material that holds the detector elements will be fabricated with carbon-fiber compounds in order to reduce the background of activation radioactivity produced by cosmic-rays in aluminum.

Performance The performance of the GRM on GRIPS in an equatorial low Earth orbit was extensively simulated with the MGGPOD suite and analyzed with the MEGAlib package. MEGAlib contains a geometry and detector description tool that was used to set up the detailed modelling of the GRM with its detector types and characteristics. The geometry file is then used by the MGGPOD simulation tool to generate artificial events. The event reconstruction algorithms for the various interactions are implemented in different approaches (Chi-square and Bayesian). The high level data analysis tools allow response matrix calculation, image reconstruction (list-mode likelihood algorithm), detector resolution and sensitivity determination, spectra retrieval, polarization modulation determination etc. Based on many billions of simulated events we have now derived a good understanding of the properties of GRIPS.

Various source and spectral scenarios have been simulated: a series of GRB spectra and intensities which span the range of burst properties known from BATSE as well as time constant line and continuum sources were simulated and analyzed. In all cases the environmental orbital radiation background and the instrumental activation were

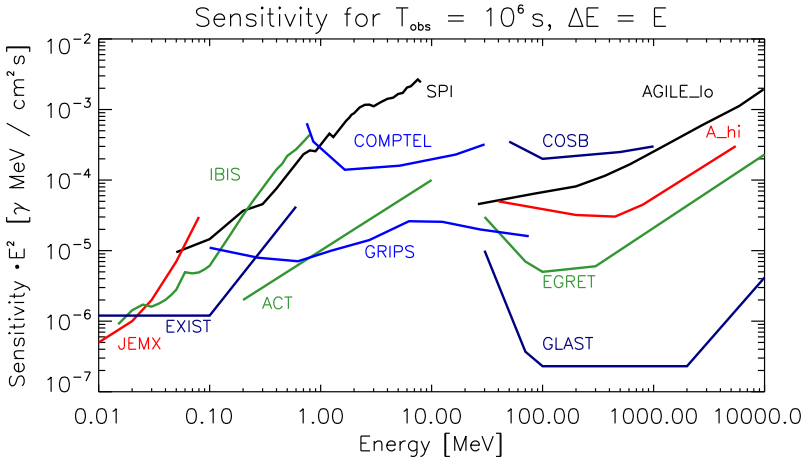

FIGURE 7. The sensitivity of the Gamma-Ray Monitor as compared to previous missions in this energy range as well as present and planned missions.

taken into account. The small intrinsic radioactivity of the proposed scintillator material $LaBr_3$ (0.8-2.0 cts/sec/cm^3 depending on the compound) is negligible compared to other background components and has been ignored in the simulations.

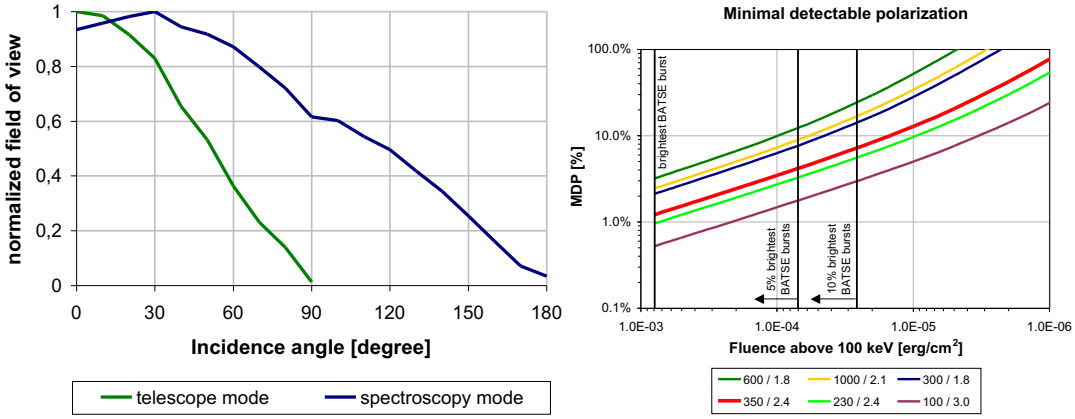

FIGURE 8. **Left:** Field of view of the Gamma-Ray Monitor. **Right:** Polarisation sensitivity of GRM. Various models of GRB spectra are shown which differ in their break energy and their high-energy powerlaw slope; see legend for the parameter pair for each model. Note that at the bright end the minimal detectable polarization changes much more slowly than the fluence. Colour codes, like 600/1.8, reads as GRB with E_{break}=600 keV, and power law photon index of 1.8 for $E \geq E_{break}$.

Continuum sensitivity: GRIPS will achieve a major improvement in sensitivity over previous and presently active missions, such as a factor 40 improvement over COMPTEL around 1 MeV, or a factor of >20 over IBIS above 200 keV. Also, GRIPS will be more sensitive than NASA's planned EXIST-mission above 250 keV (Fig. 7). The FOV, simulated for a typical GRB spectrum (Fig. 8, left panel) extends to large off-axis angles: in "telescope-mode" up to $\sim 50^\circ$ incidence angle for the 50% level, or all-sky in "spectroscopy-mode".

Line sensitivity: For the standard operation mode, the all-sky scan, the resulting sensitivity is slightly worse than in pointing mode since the exposure is distributed over most of the sky and not concentrated into a small FOV like for INTEGRAL. This reduction is, however, offset by the large geometrical factor (effective area $\times$ solid angle), the uniformity of the scan, and the permanent accumulation of exposure. As consequence, after 5 years in orbit, GRIPS will achieve a factor 40 sensitivity improvement at the 1809 keV line, over COMPTEL's sensitivity achieved for 9 yrs exposure.

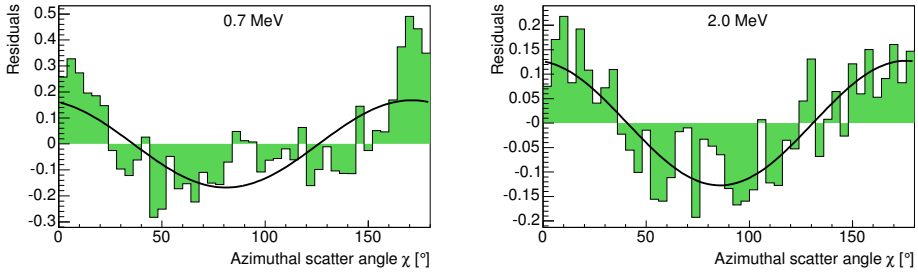

FIGURE 9. Measured polarisation response of the MEGA prototype for two different energies. Within measurement errors and statistics, all values are in agreement with GEANT4 simulations: the polarisation angle of 90° is reproduced to 82%±24% (0.7 MeV) and 86%±11% (2.0 MeV), respectively. The measured modulation is 0.17±0.04 and 0.13±0.03 as compared to the simulated values 0.19 (at 0.7 MeV) and 0.14 (2.0 MeV). (From Zoglauer 2005)

Polarisation: The dominant mode of interaction for photons in Silicon in the energy range from a few hundred keV to about 8 MeV is Compton scattering. Linearly polarised γ–rays preferentially scatter perpendicular to the incident polarisation vector, resulting in an azimuthal scatter angle distribution (ASAD) which is modulated relative to the distribution for unpolarised photons. The sensitivity of an instrument to polarisation is given by the ratio of the amplitude of the ASAD and its average, which is called the modulation factor μ. The modulation is a function of incident photon energy, E, and the Compton scatter angle, θ, between the incident and scattered photon directions (see Fig. 9 for the MEGA calibration).

GRIPS is a nearly perfect polarimeter (Fig. 8, right panel): The well-type geometry allows the detection of Compton events with large scatter angles which carry most of the polarisation information. GRIPS' polarisation sensitivity will be best at 200–400 keV where the polarisation information of the photons is best preserved through the Compton scatter process.

Gamma-ray Bursts: We have created model spectra with parameters for $E_{\rm peak}$, high-energy power law slope β and peak flux, which cover the distribution of these parameters as observed with BATSE (4th BATSE catalog; Paciesas et al. 1999). The faintest BATSE GRBs are clearly 'detected' by GRIPS with spectra extending from 100 keV up to 2 MeV and having more than 7 energy bins with 3σ each. From these simulations we estimate that GRIPS will be a factor of 3 more sensitive than BATSE below 1 MeV and detect about a factor of 2.5 more GRBs than BATSE. Folding in the smaller field of view of GRIPS compared to BATSE, we find that GRIPS will detect 665 GRBs/yr. For GRBs at an off-axis angle of $>70^\circ$, only poor localizations, if any, will be possible, so we expect 440 GRBs/yr with good positions and XRM follow-up.

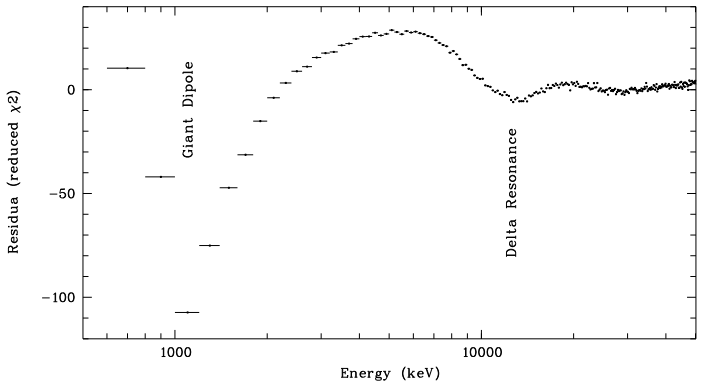

FIGURE 10. Residuals of a simulated power law spectrum with resonance absorption and the model fit with a straight power law. The GRB was chosen among the 3% brightest BATSE bursts, with 10 sec duration, and an intervening rest-frame column of 5×10^{26} cm^{-2}. The spectrum has been sent through the full GRM detector model. The power law slope is reproduced to within 0.1, and the resonance lines (marked) are detected at overwhelming significance.

With 665 GRBs per year, and a nominal lifetime of 5 yrs (goal 10 yrs) we would expect 33–330 (goal 66–660) GRBs at z>10, and 3–33 GRBs (goal 6–66) at z>20. Of these, 67% would be detected with an accurate (<25 arcsec) position. This estimate includes a duty cycle of the instrument similar to that of BATSE and a detection rate of the X-ray afterglows of 98%, as for Swift/XRT. (We note for comparison that Naoz & Bromberg (2007) predict 1% of GRBs at z>20 in their pessimistic case and 5% and 15% for their optimistic cases.) This implies that (1) the detection frequency of GRBs at z>20 is high enough to achieve at least one detection during the mission lifetime, and (2) that GRIPS will clearly detect the cut-off in the z-distribution IF star formation starts at a certain redshift (below $\sim$25) throughout the Universe. (Even if this cut-off were to happen at $z < 13$, it would be a very important measurement.) Measuring this cut-off up to $z\sim$25, would in turn be a limit to the earliest time when stars formed and re-ionization might have happened.

X-ray telescope

The main driver for the design of the X-ray monitor (XRM) is the positional accuracy of GRBs, so that their full error circle can be covered by the XRM. GRM will determine GRB positions to better than 1° (radius, 3σ) down to off-axis angles of 60°. We add a 50% margin, and require a field of view of the XRM of 3° diameter.

The second requirement is for sensitivity which should be at least a factor 3 larger than that of Swift's XRT, since GRIPS will cover more distant GRBs, and thus likely fainter afterglows. Such sensitivity requirement (of order >300 cm^2) excludes coded mask systems, and even single-telescope Wolter-I optics are problematic.

The most cost-effective option is to adopt the eROSITA scheme of 7 Wolter-I telescopes and adjust their orientation on the sky such that they fill the required FOV.

eROSITA (for **e**xtended **RO**entgen **S**urvey with an **I**maging **T**elescope **A**rray) (Predehl et al. 2006) shall perform the first imaging sky survey in the medium X-ray range, i.e. between 0.2 and 12 keV. Similar to the XMM EPIC/PN, the eROSITA detectors will share the high quantum efficiency (>90% over 0.2-10 keV band), the high radiation hardness against high energy protons including self-shielding against the low energy protons focused by the Wolter telescope. But eROSITA detector will have a number of improvements over the XMM EPIC/PN detector: (i) lower noise, (ii) smaller charge transfer losses, (iii) higher energy resolution, (iv) smaller number of out-of-time events, (v) better time resolution. The effective area of the eROSITA telescope well matches the GRIPS requirements.

For some fraction of the mission, the XRM would perform follow-up observations of GRB afterglows. Over one year of mission time, about 10% of the sky would be covered with an exposure time of typically 20 ksec, thus reaching a flux of about 4×10^{-15} erg/cm^2/s. For 10 yrs mission life time, the whole sky would be covered to this limit.

REFERENCES

1. Abel T., Wise J.H., Bryan G.L., 2007, ApJ 659, L87
2. Amati L., et al. 2002, A&A, 390, 81
3. Andritschke R., 2005, Exp. Astron. 20, 395
4. Arav N., Kaastra J., Steenbrugge K., et al., 2003, ApJ 590, 174
5. Arav N., Kaastra J., Kriss G.A., et al., 2005, ApJ 620, 665
6. Bate M.R., Bonnell I.A., Bromm V., 2003, MNRAS 339, 577
7. Boggs S.E., Coburn, W., Kalemci, E., 2006, ApJ 638, 1129
8. Branch D., Nomoto K., 2007, Nature, 447, 393
9. Bromm V., Loeb A., 2002, ApJ 575, 111
10. Bromm V., Loeb A., 2006, ApJ 642, 382
11. Cheng K.S., Chernyshov D.O., Dogiel V.A., 2006, ApJ 645, 1138
12. Diehl R., et al. 2006, Nature 439, 45
13. Elitzur M., Nenkova M., Ivecic Z., 2004, in "The Neutral ISM in Starburst Galaxies", Eds. S. Aalto, S. Huttemeister, A. Pedlar, ASP 320, p. 242
14. Gao L., Yoshida N., Abel T., Frenk C.S., Jenkins A., and Springel V., 2007, MNRAS 378, 449
15. Ghirlanda G., Ghisellini G., Lazzati D., 2004, ApJ 616, 331
16. González M.M., Dingus B.L., Kaneko Y., et al., 2003, Nature 424, 749
17. Granot J., Königl A., 2003, ApJ 594, L83
18. Granot J., 2003, ApJ 596, L17
19. Greiner J., Iyudin A., Kanbach G., et al., 2008, Exp.Astr., in press
20. Hartman, R.C., Bertsch, D.L., Bloom, S.D. et al. 1999, ApJS 123, 79
21. Harding A.K., 2007, AIPC-921, 226
22. Heger et al. 2003, ApJ, 591, 288
23. Homeier N.L., 2005, ApJ 620, 12
24. Hooper D., Wang L., 2004, Phys. Rev. D., 063506
25. Iyudin A.F., Diehl R., Bloemen H. et al. , 1994, A&A 284, L1
26. Iyudin A.F., Reimer O., Burwitz V., Greiner J., Reimer A., 2005, A&A 436, 763
27. Iyudin A.F., Burwitz V., Greiner J., Larsson S., Küpcü Yoldas A., 2007a, A&A 468, 919
28. Iyudin A.F., Greiner J., Larsson S., Ryde F., 2007b, in "Gamma-Ray Bursts: Prospects for GLAST", Sept. 2006, Eds. M. Axelsson and F. Ryde, AIPC-906, p. 89
29. Jiang Z.L., Zhang L., 2006, ApJ 642, 1130
30. Jorstad S.G., Marscher A.P., Lister M.L. et al. 2006, ASP CS-350, 149
31. Knödlseder J., et al., 2005, A&A 441, 513
32. Kogut A., Spergel D.N., Barnes C. et al 2003, ApJS 148, 161
33. Kuiper L., Hermsen W., den Hartog P.R., Collmar W., 2006 ApJ 645, 556

34. Lamb D.Q., Reichart D.E., 2001, in *GRBs in the afterglow era*, eds. Costa et al. ESO-Springer, p. 226
35. Leibundgut B., 2001, ARA&A 39, 67
36. Limongi M., Chieffi A., 2006, ApJ, 647, 483
37. Lyutikov M., Pariev V.I., Blandford R.D., 2003, ApJ 597, 998
38. McBreen S., Hanlon L., McGlynn S. et al. 2006, A&A 455, 433
39. Mészáros P., 2006, Rep. Prog. Phys. 69, 2259
40. Naoz S., Bromberg O., 2007, MNRAS 380, 757
41. Paciesas W.S., Meegan C.A., Pendleton G.N., et al.1999, ApJS 122, 465
42. Pavlinsky M., Hasinger G., Parmar A., Fraser G., Churazov E. et al. 2006, SPIE 6266, 18
43. Pe'er A., Waxman E., 2004, ApJ 613, 448
44. Porter T.A., Moskalenko I.V., Strong A.W. et al., 2008, ApJ (in press; arXiv:0804.1774)
45. Prantzos N., 2004, A&A, 420, 1033
46. Prantzos N., Diehl R., 1996, Phys. Rep. 267, 1
47. Predehl P., Hasinger G., Böhringer H., Briel U., Brunner H. et al. 2006 SPIE 6266, 19
48. Rees M.J., Mészáros P., 2005, ApJ 628, 847
49. Ryde F., 2005, ApJ 625, L95
50. Schady P., Mason K.O., Page K., et al. 2007, MNRAS 377, 273
51. Schönfelder, V. Bennett, K., Blom, J.J. et al. 2000, A&AS 143, 145
52. Sim S.A., Mazzali P.A., 2008, MNRAS 385, 1681
53. Spolyar D., Freese K., Gondolo P., 2008, PRL 100, 051101
54. Starling R.L.C., Wijers R.A.M.J., Hughes M.A. et al. 2005, MN 360, 305
55. Steidel C.C., et al. 1999, ApJ 519, 1
56. Story S.A., Gonthier P.L., Harding A.K., 2007 ApJ, 671, 713
57. Strong A.W. et al. 2005, A&A 444, 495
58. Tatischeff V., Kozlovsky B., Kiener J., Murphy R.J., 2006, ApJS 165, 606
59. The L.-S., Clayton D.D., Diehl R. et al. 2006, A&A 450, 1037
60. Varier K.M., Nasiruddeen Kunju M.A., Madhusudanan K., 1986, Phys.Rev. A33, 2378
61. Vink J., Laming J.M., Kaastra J.S., et al. 2001, ApJ 560, 79
62. Vreeswijk P.M., Ledoux C., Smette A., et al. 2007, A&A 468, 83
63. Wang W. et al. 2007, A&A (in press; arXiv:0704.3895)
64. Wehrle A.E., Piner B.G., Unwin S.C. et al. 2001, ApJS 133, 297
65. Weidenspointner G., et al. 2005, ApJS 156, 69
66. Woosley S.E., Weaver T.A., 1995, ApJS 101, 181
67. Woosley S., et al 2006, AIP 836, 398
68. Yoon S.-C., Langer N., Norman C.A., 2006, A&A, 460, 199
69. Yoshida N., Bromm V., Hernquist L., 2004, ApJ 605, 579
70. Yoshida N., Omukai K., Hernquist L., Abel T., 2006, ApJ 652, 6
71. Zoglauer A., 2005, PhD thesis, TU Munich
72. Zoglauer A., Andritschke R., Schopper F., 2006, New Astron. Rev. 50, Issues 7/8, 629